International Journal of Advanced Computer Technology (IJACT)
ISSN:2319-7900

Computer Aided Hard Exudates Detection on Digital Fundus Images Using Morphology and Multi-resolution Analysis

Poonam M.Rokade, Dept. of CS & IT, Dr.B.A.M.U.,Aurangabad (MS); R.Manza, Dept. of CS & IT, Dr.B.A.M.U.,Aurangabad (MS); Prabhat Jonathan, Member of Technical Staff CDAC, Aurangabad

Abstract

Here Diabetic Retinopathy (DR) is one of the leading epidemiology of vision loss caused by the implications of diabetes. Therefore, retinal health monitoring of diabetic patient is significant for prevention of vision loss. Hard exudates (HEx) are one of the most occurring lesions in DR caused by vascular damage with leakage. They are yellowish or white patches, varying sizes, shapes, and locations. This paper represents, the automated detection of HEx using morphological techniques and multi-resolution analysis. The Haar Dual Tree Wavelet Transform is used in these techniques. The classification is done using KNN. Here, we obtained highest results for MISP database as sensitivity 0.75%, specificity and PPV 1%, NPV is 0.28% and accuracy 0.77%. Whereas, lowest sensitivity and accuracy is obtained for DB1 database as 0.26% and 0.3% respectively and specificity achieved 1% for all databases.

Keywords: DR, Retinal images, Multi-resolution analysis, Wavelet Transform, KNN classifier.

I. Introduction

Diabetic retinopathy (DR) is retinopathy (damage to the retina) caused by implications of diabetes [1]. It is considered to be the result of vascular changes in the retinal circulation. These abnormalities in the retina are due to insufficient insulin in the body [1], [2]. The progressive eye disease begins as non-proliferative retinopathy and progress to severe non-proliferative retinopathy by growth of new blood vessels in and on the retina and even on the iris. The WHO reported that, in recent years, DR is leading cause of vision loss [3], [4] that currently affects 250 million of people worldwide [5]. Hence early detection of DR is crucial for prevention of vision loss and to monitor the health of the retina for those people who have signs of DR [6]. Therefore diabetic patients require regular medical checkup for effective timing of sight saving treatment [7].

Non-proliferative DR (NPDR) is the most common type of DR; develop at any point in time after the onset of diabetes. Exudates are one of the most commonly occurring lesions among DR lesions. These are either seen as individual spots, clusters, or are found in large rings around leaking capillaries. If the lipid extends into the macula area, vision can be severely compromised. The detection and quantification of exudates will significantly contribute to the mass screening and assessment of NPDR [7], [8]. (See fig.1) Although exudates may absorb spontaneously, they usually tend to increase in volume in an untreated retina. Automated and robust screening system for DR detection can effectively reduces the burden of the specialist and saves cost as well as time. Retinal imaging is widely used by ophthalmologists to screen for epidemic eye diseases such as DR. Color fundus photography (CF) provides a high sensitivity for a wide range of diabetic retinal changes two dimensionally [9]. Their digital nature allows automatic analysis to reduce the workloads of the ophthalmologists and the health costs in the screening of the disease [2]. The eye fundus is sensitive to vascular diseases so fundus imaging consider as a candidate for non-invasive screening. The success of this type of screening approach depends on accurate fundus image capture and especially on accurate and robust image processing and analysis algorithms for detection of abnormalities [10] with improving sensitivity and specificity. (See fig.1).

II. Survey of Literature

The second aspect is the survey of literature of exudates detection. Among the literatures, the technique used by **Alireza Osareh**, **et al., 2001** is Fuzzy C-Means clustering and neural network (NN) to classify regions into exudates and non exudates patches. They achieve 92% sensitivity

ISSN:2319-7900

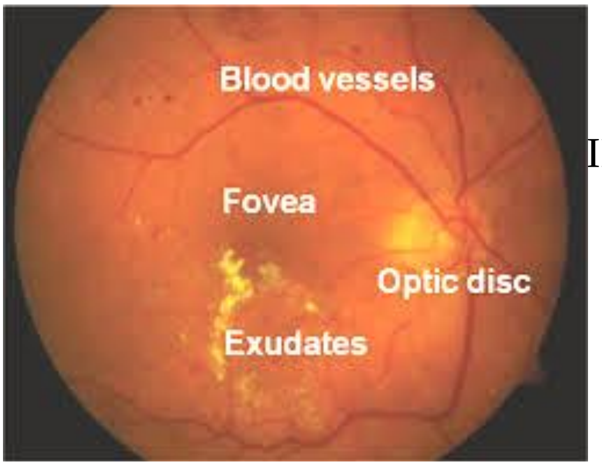

Fig.1.Retinal image with main features

and 82% specificity [13]. **Thomas Walter, et al., 2002,** used Histogram Equalization techniques and Fuzzy C-means Clustering algorithm. They obtained sensitivity 80% and specificity 99.5% [14]. The morphological transformation approach was used by **Harihar Narasimha Iyer, et al., 2007,** for preprocessing followed by neural network system technique. They got sensitivity 94.78% and specificity 94.29% [15]. **Clara I. Sanchez, et al., 2009,** used Mixture models algorithms to dynamically threshold the images in order to separate exudates. They obtained 90% sensitivity and 96.8% positive predictive value (ppv) in exudates detection [6]. **Hussain F. Jaafar** used Split and Merge algorithm for exudates detection. He achieved sensitivity 89.7%, specificity 99.3% and accuracy 99.4% [2]. **Luca. Giancardo et al., 2011,** introduced methodology for diagnosis of DME based on three feature vectors i.e. Exudate probability map, Color analysis and Wavelet analysis. The algorithm obtained an AUC (Area Under the ROC Curve) between 0.88 and 0.94 [16]. **Hussain F., et al., 2011,** proposed an automated algorithm to detect and grade the severity of hard exudates. The results obtained with sensitivity of 93.2%, PPV (Positive Predictive Value) of 80.7%, specificity of 99.2% and accuracy of 99.4% [17]. **Atul Kumar et al., 2012**, used **SVM** (Support Vector Machine) with morphological operation to detect exudates. The sensitivity of method is 97.1% and the specificity is 98.3% [18]. **R.Radha and Bijee Lakshman; 2013,** developed a method to recognizes the retina to be

normal or abnormal. They got 98% accuracy in the detection of the exudates in the retina [19]. **A. Osareh, et al., 2003,** used the Fuzzy C-means clustering and neural network. It demonstrates 93.0% sensitivity and 94.1% specificity in terms of exudates based classification [20]. **R. F. Mansour, et al., 2013,** us Discrete Cosine Transform (DCT) analysis and SVM classifier for retinal exudates detection. The system achieved accuracy with 97.0% sensitivity and 98.7% specificity [21].

III. Proposed System

In proposed approaches, retinal hard exudates are detected by using morphological operations and multi-resolution analysis tools i.e. wavelet transform. The classification is done by using KNN classifier. In quantitative evaluation slightly different results obtained while applied segmentation, sobel edge detection and wavelet transform in the way that images run one by one and image database run at a time.

A. Morphological Operations

In this approach, we have used some morphological operations for geometrical transformations, color normalization, and contrast enhancement for pre-processing. Therefore, we can get the exudates probability map. Here, green channel of the image is used because of its high intensity as compared to red and blue [22]. The images are resized to a height of 720 pixels maintaining the original height/width ratio. The mathematical formula for finding green channel is given below:

$$g = \frac{G}{R+G+B} \qquad (1)$$

Here, g→ green channel

R, G, B→ Red, Green, Blue respectively.

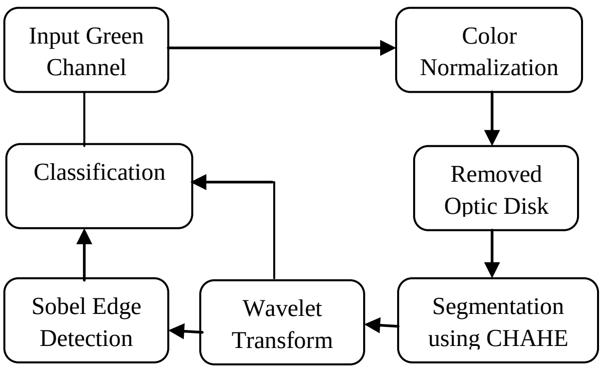

Fig.2. Process flow for Exs detection using Morphological operations

1. Color Normalisation

Due to intra-image and inter-image variability in the retinal color in different patients, it is necessary to normalize the color. Optic disk is removed from an image using non-flat structuring element [22]. It

ISSN:2319-7900

might be mistaken as exudates, if it is not segmented and masked out [6]. Mathematical expression for histogram equalization technique of the standard image is given below. Let Ps(s) and Pd(s) represent the standard image and desired image probability density functions, respectively.

$$u = T(s) = \int_0^s p_s(x)dx \qquad (2)$$

2. Contrast Enhancement

The Contrast–Limited Adaptive Histogram Equalization (CLAHE) algorithm is used to make an object distinguishable from other objects and background. So the resulted image would have uniform background and high contrast. Hence exudates detected clear due to converting reference image into binary image or threshold.

3. Wavelet Transform

It is powerful tool for multi-resolution analysis. Here, we apply Haar wavelet transform on reference (threshold) image for decomposition and reconstruction in order to get more accuracy in exudates detection. Hence, the reconstructed image has been used to classify an image into with exudates and non-exudates image.

4. Sobel Edge Detection Operator

This operator is used for exudate boundary detection only. Here, we have got different results in parameters (area and quantity) of exudates rather than in detection using wavelet transform. Therefore, these are also used in statistical analysis. Figure 3 shows images obtained after applying morphological operation, whereas in figure 4 only exudates boundaries are detected. (See fig.3).

B. Multi-resolution Analysis Tool

Haar wavelet transform is of orthogonal wavelet family. It is important tool for image denoising due to its energy compaction property [23]. It can keep the track of time and frequency information. Wavelet transform computes approximation coefficient matrix and details coefficient matrices i.e. horizontal, vertical and diagonal respectively. In this approach, we have reduced some steps for exudates detection. Wavelet decompositions allow for very good image approximation with just a few coefficients and described at different levels of resolution. This property has been exploited for lossy image compression [24]. Wavelet decompositions can be used to extract and encode edge information [25]. The coefficients of wavelet decomposition provide information that is independent of the original image resolution. Thus, a wavelet-based scheme allows the resolutions of the query and the target to be effectively decoupled. Wavelet decompositions are fast and easy to compute, requiring linear time in the size of the image and very little code [26]. See fig.4 for data flow.

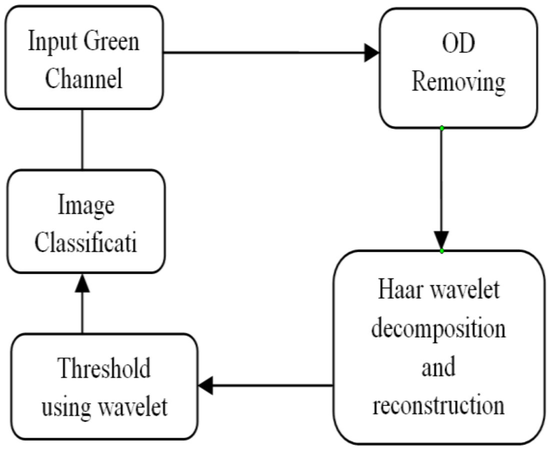

Fig.4. Process flow for multi-resolution analysis

$HT^n(f)$ of an N-input function $X^n(f)$ is the 2^n element vector.

$$HT^n(f) = H^n X^n(f) \qquad (3)$$

It is performed in levels. At each level, the Haar transform decomposes a discrete signal into two components with half of its length: an approximation (or trend) and a detail (or fluctuation) component. The first level of approximation $\boldsymbol{a}^1=(a_1,a_2,\cdots,a_{N/2})$ is defined as

$$a_m = \frac{X_{2m-1} + X_{2m}}{\sqrt{2}} \qquad (4)$$

For m=1,2,3,⋯,N/2, where X is the input signal. The multiplication of $\sqrt{2}$ ensures that the Haar transform preserves the energy of the signal. The values of $\boldsymbol{a}^1$ represent the average of successive pairs of X value.

The first level of detail $\boldsymbol{d}1=(d1, d2,\cdots, d_{N/2})$ is defined as

$$d_m = \frac{X_{2m-1} + X_{2m}}{\sqrt{2}} \qquad (5)$$

ISSN:2319-7900

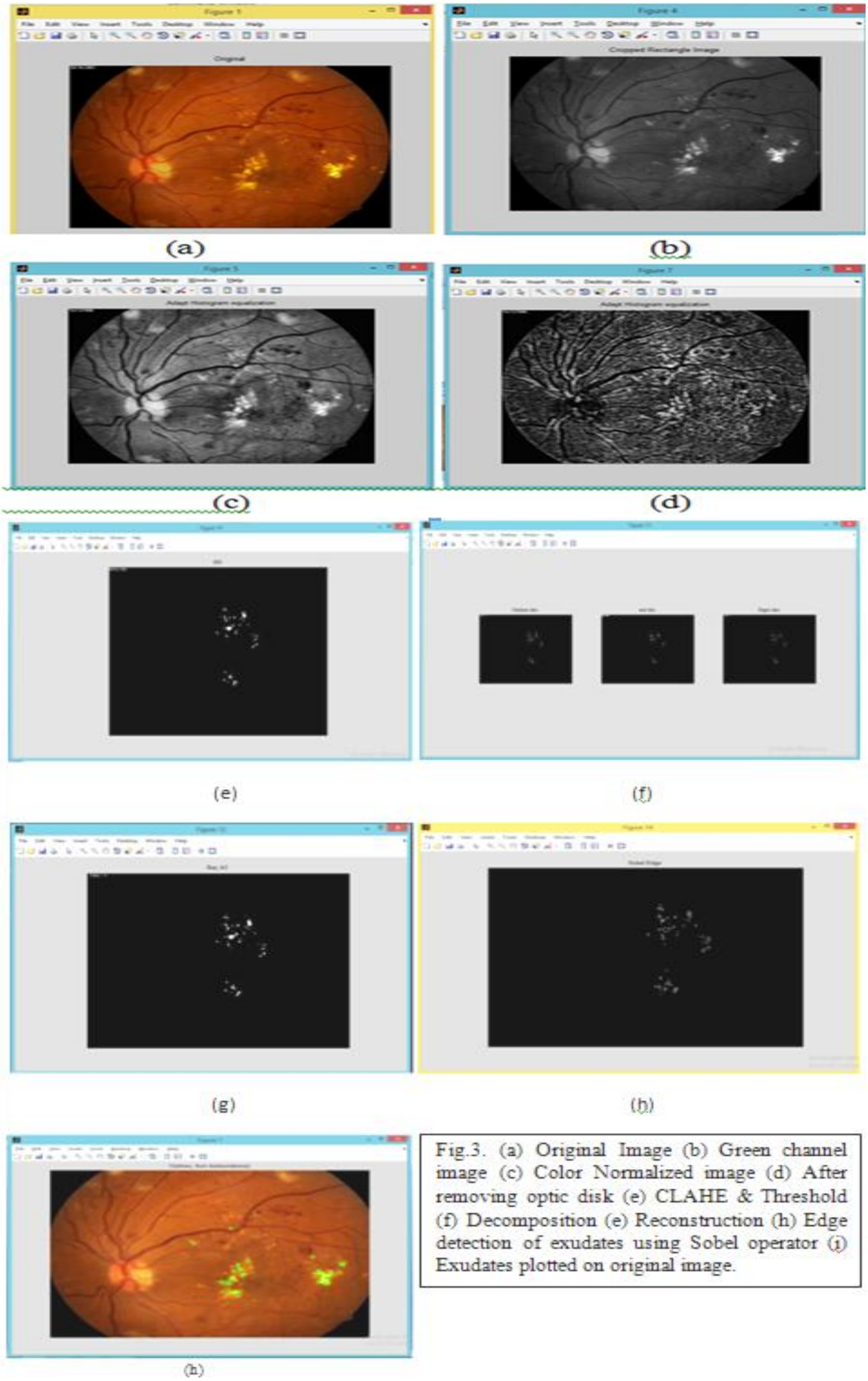

Fig.3. (a) Original Image (b) Green channel image (c) Color Normalized image (d) After removing optic disk (e) CLAHE & Threshold (f) Decomposition (e) Reconstruction (h) Edge detection of exudates using Sobel operator (i) Exudates plotted on original image.

Fig.3.Images after applying Morphological operations

ISSN:2319-7900

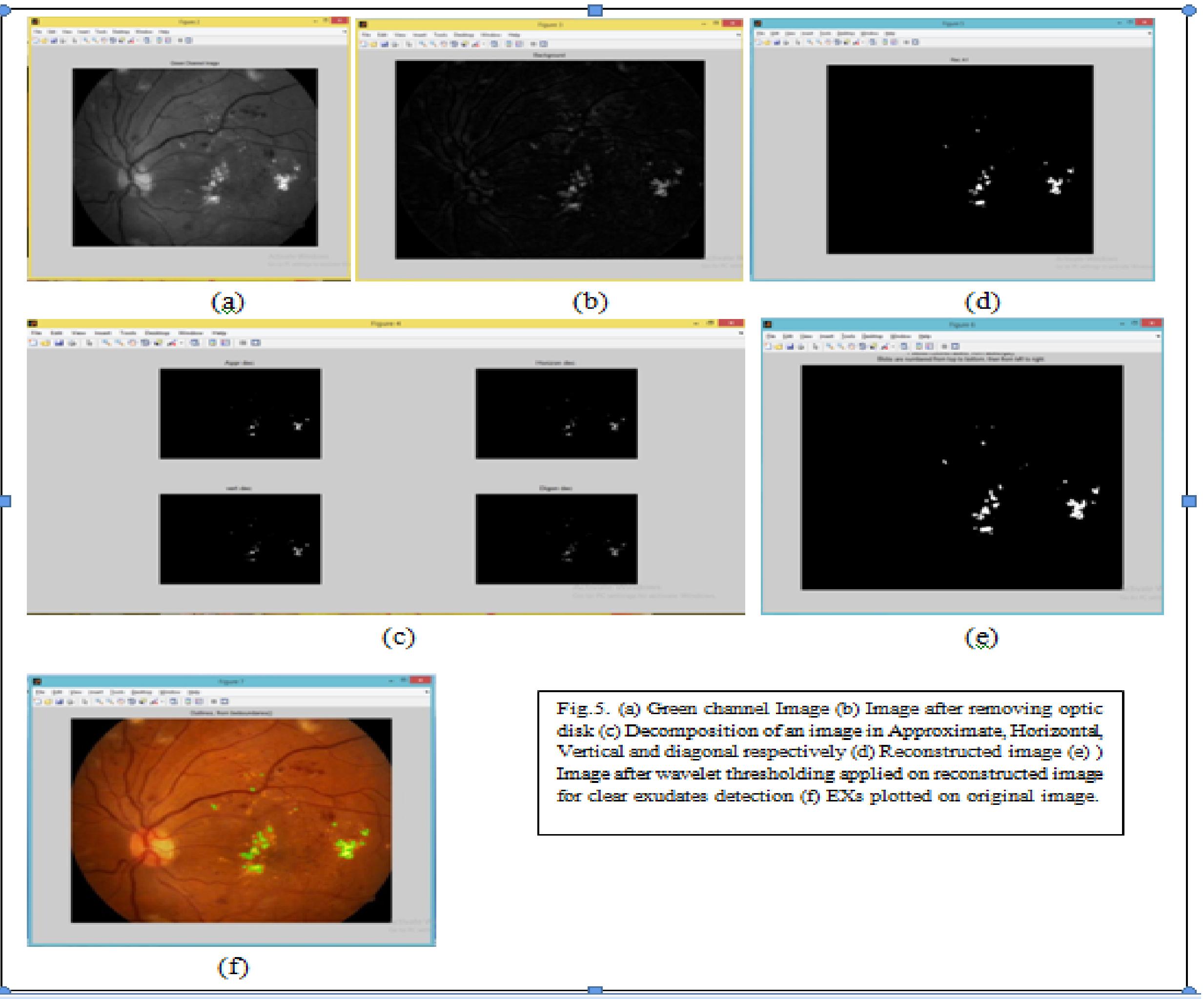

Fig.5. (a) Green channel Image (b) Image after removing optic disk (c) Decomposition of an image in Approximate, Horizontal, Vertical and diagonal respectively (d) Reconstructed image (e)) Image after wavelet thresholding applied on reconstructed image for clear exudates detection (f) EXs plotted on original image.

Fig. 5 that shows exudates appears brighter than in previous experiment with less steps applied.

The values of d^1 represent the difference of successive pairs of X value.

The inverse of this transformation can be achieved by

$$X = \frac{a_1+d_1}{\sqrt{2}}, \frac{a_1-d_1}{\sqrt{2}}, \ldots \frac{a_{N/2}+d_{N/2}}{\sqrt{2}}, \frac{a_{N/2}-d_{N/2}}{\sqrt{2}} \qquad (6)$$

IV. Classification

Here, K-Nearest-Neighbor classifier is used to check number of correctly classified images into exudates and non-exudates. It is an instance-based. It delays the process of modeling the training data until it is needed to classify the test samples. It can be used both for classification and prediction. The training samples are described by n-dimensional numeric attributes. Here, 35 training datasets are used. The training samples are stored in an n-dimensional space. When a test sample (unknown class label) is given, the KNN classifier searches the k training samples which are closest to the unknown sample. Closeness is usually defined in terms of Euclidean distance. The Euclidean distance is between two points P(p1,p2,…. Pn) and Q(q1,q2,…. qn) given by equation 7.

$$d(P,Q) = \sqrt{\sum_{i=1}^{n} (p_i - q_i)^2} \qquad (7)$$

KNN classifier is very simple to implement and easy to justify the outcome of KNN.

V. Evaluation

Quantitative evaluation of the segmentation algorithm is done by calculating the sensitivity and specificity using exudates area and the number of exudates. It has been given different results while run

ISSN:2319-7900

images one by one and image database run at a time. See table no.1 for performance evaluation.

Table 1. Performance Analysis

		Ground Truth	
		Positive	Negative
	Positive	Truth Positive (TP)	False Positive (FP)
Method Result	Negative	Truth Negative (TN)	False Negative (FN)

Using this table, sensitivity and specificity are evaluated (see eq.8, 9). Sensitivity is the percentage of abnormal fundus images classified as abnormal, and specificity is the percentage of normal fundus images classified as normal by the screening. The higher the sensitivity and specificity values, the better the diagnosis. Formula to calculate Sensitivity and specificity is as:

$$\text{Sensitivity} = \frac{TP}{TP+FN} \qquad (8)$$

$$\text{Specificity} = \frac{TN}{TN + +FP} \qquad (9)$$

Graph 1.

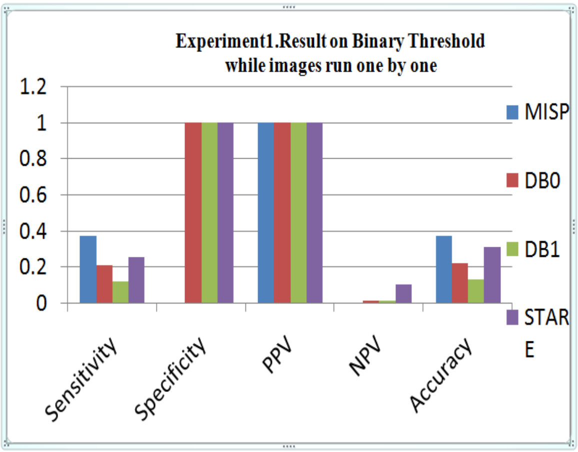

Graph 2.

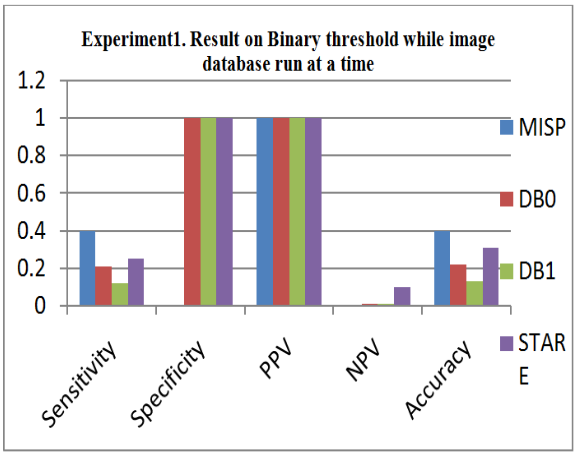

Graph 3.

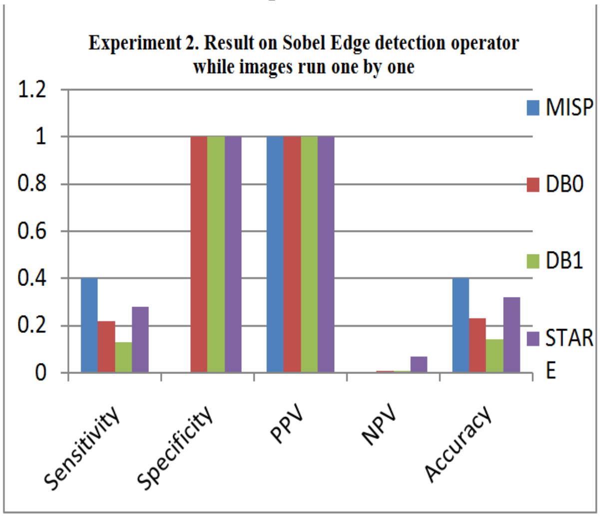

Graph 4.

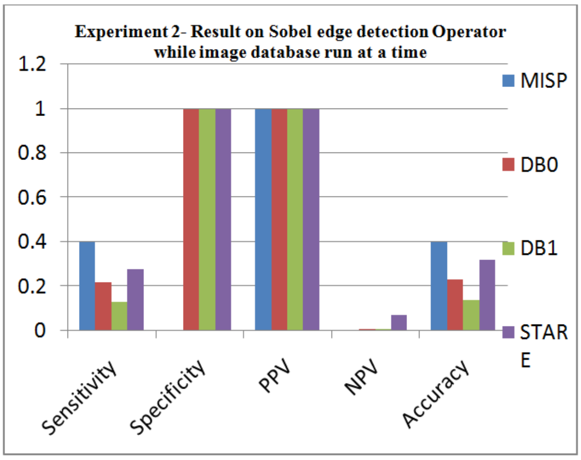

ISSN:2319-7900

Graph 5.

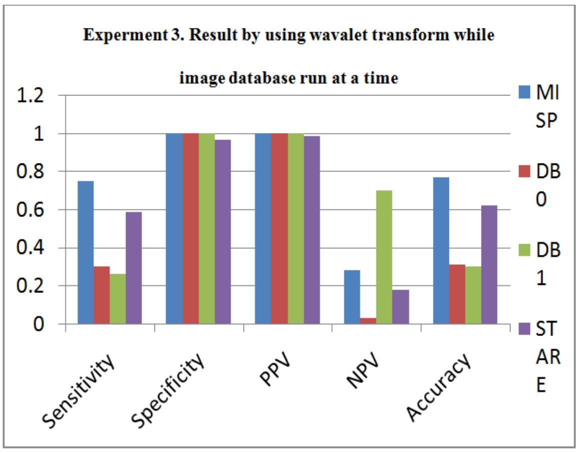

The above graphs shows obtained sensitivity, specificity, PPV, NPV, and accuracy for databases MISP, DB0, DB1 and STARE in order to images run separately and image database run at a time.

VI. Results and Conclusions

In these experiments we have obtained highest sensitivity, specificity, PPV, NPV and accuracy as 0.75%, 1%, 1%, 0.28% and 0.77% respectively for MISP database by using Haar wavelet transform for multi-resolution analysis. Whereas by using binary threshold and sobel edge detection operator the specificity and NPV for MISP database is obtained 0%. The lowest sensitivity accuracy is obtained for DB1 database as 0.26% and 0.3% respectively. When images run one by one and image database run at a time, slightly different results obtained in sensitivity, specificity, NPV, PPV, accuracy.

Using Haar wavelet transform tool, exudates can be detected by using minimum steps applying. In future, we will try to improve the sensitivity and specificity, also the PPV, NPV and accuracy using other orthogonal wavelet family.

REFERENCES:

[01] Atul Kumar, et al., “A Segment based technique for detecting exudate from Retinal Fundus Image”, Procedia Technology 6(2012), 2nd International Conference on Communication, Computing & Security, pp. 1-9, 2012.

[02] Hussain F., et al., “Automated Detection of exudates in Retinal Images Using A Split-And-Merge Algorithm”, 18th European Signal Processing Conference (EUSIPCO-2010), Aalborg, Denmark, August 23-27, ISSN 2076-1465, 2010.

[03] Shirin Hajeb Mohammad Alipour, et al., “Diabetic Retinopathy Grading by Digital Curvelet Transform”, Hindawi Publishing Corporation, Computational and Mathematical Methods in Medicine, Volume 2012, Article ID 761901, 11 pages, doi:10.1155/2012/761901.

[04] Aiello, L.P., Cahill, M.T., andWong, J.S., Systemic considerations in the management of diabetic retinopathy, Am J Ophthalmol, 132, 760, 2001.

[05] Nguyenl, H.T. at el., “Classifation of Diabetic Retinopathy using Neural Networks”, Engineering in Medical and Biology Society, 18th Annual International Conference of the IEEE, Oct. 31-Nov. 3, Amsterdam, pp: 1548-1549, DOI: 10.1109/IEMBS.1996.647546.

[06] Clara I. Sánchez, et al., “Retinal image analysis based on mixture models to detect hard exudates”, Medical Image Analysis, pp. 650–658, doi:10.1016/j.media.2009.05.005, 2009.

[07] Carla Agurto, et al., “Detection of Hard Exudates and Red Lesions in the Macula Using a Multiscale Approach”, SSIAI 2012, 978-1-4673-1830-3/12, IEEE, 2012.

[08] Kanski, J., Diabetic Retinopathy, Clinical Ophthalmology, Butterworth-Heinmann, Oxford, UK, 1997.

[09] Jan Lammer, et al., “Detection and Analysis of Hard Exudates by Polarization- Sensitive Optical Coherence Tomography in Patients With Diabetic Maculopathy”, IOVS, Vol. 55, No. 3, ISSN: 1552-5783, March 2014.

[10] Pavle Prenta, “Detection of Diabetic Retinopathy in Fundus Photographs”, University of Zagreb, Faculty of Electrical Engineering and Computing, Unska 3, 10000, Zagreb, Croatia.

[11] M. Zikos, E. Kaldoudi, S. C. Orphanoudakis, “DIPE: A Distributed Environment for Medical Image Processing”, Studies in Health Technology and Informatics, vol. 43, Pt. B, pp. 465-469, 1997.

[12] Thomas M. Deserno, Til Aach, at el., “Advances in medical image processing”, Computer Science Res Dev, Springer Verlag pp.1–3, DOI 10.1007/s00450-010-0142-0, 2011.

[13] Alireza Osareh, et al., “Auomatic Recognition of Exudative Maculopathy using Fuzzy C-Means Clustering and Neural Networks”,

Medical Image Understanding and analysis, E. Claridge, J. Bamber, (eds), pp.49-52, July 2001.

[14] Thomas Waleter, et al., "Automatic Detection of Microaneurisms in color fundus images of the Huma Retina by means of the Bounding Box Closing", COLOSIMA, A. GIULIANI, A.SIRABLLA, P.: Lecture Notes in Computer science, LLNCS, vol. 2526, p.210-220, Spinger-Verlag, October 2002.

[15] Harihar Narasimha Iyar, et al., "Automatic Identification of retinal arteries and vins from dual-wavelength images using structural and functional features ", IEEE Trans. Biomedical Eng. 54(8), pp.1427-35, Aug 2007.

[16] Luca Giancardo, et al., "Automatic retina exudate segmentation without a manually labelled training set", Biomedical Imaging, IEEE, pp.1396-1400, 2011.

[17] Hussain F. Jaafar, et al., "Automatic detection and grading of hard exudates from retinal fundus images", 10th European Signal Processing Conference, Barcelona, Spain, Aug 29-Sep2, 2011.

[18] Atul Kumar et al., "A Segment based technique for detecting exudate from Retinal Fundus Image", Procedia Technology 6(2012), 2nd International Conference on Communication, Computing & Security, pp. 1-9, [ICCCS-2012].

[19] R. Radha, Bijee Lakshman, "Retinal Image Analysis Using Morphological Process and Clustering Technique", Signal & Image Processing: An international Journal (SIPIJ) Vol.4, No.6, December 2013.

[20] A. Osareh1, et al. "Automated identification of diabetic retinal exudates in digital colour images", Br J. Ophthalmol, 87:1220-122, doi:10.1136/bjo.87.10.122, 2003.

[21] R. F. Mansour, et al., "Identification of Diabetic Retinal Exudates in Digital Color Images Using Support Vector Machine", JILSA, Vol.4, No.3, ID: 35391, pp.8, 2013.

[22] Manjiri B. Patwari, et.al., "Calculation of Retinal Blood Vessels Tortuosity by using Image processing Techniques and Statistical Techniques ", 2nd International conference on System Modeling & Advanced in Research Trends (SMART), 2013.

[23] Grossman, A. and Morlet, J., "Decomposition of Hardy Functions into Square Integrable Wavelets of Constant Shape"., SIAM Journal of Mathematical Analysis, Vol. 15, No. 4, pp. 723-736,1984.

[24] R. DeVore, B. Jawerth, and B. Lucier, "Image compression through wavelet transforms coding", IEEE Transactions on Information Theory, 38(2):719–746, March 1992.

[25] Stephane Mallat and Sifen Zhong, "Wavelet transform maxima and multiscale edges", In Ruskai, et al, editor, Wavelets and Their Applications, pages 67–104, Jones and Bartlett Publishers, Inc., Boston, 1992.

[26] Charles E. Jacobs, "Fast Multi-resolution Image Querying", 22nd annual conference on Computer graphics and interactive techniques, ISBN: 0-89791-701-4, doi:10.1145/218380.218454, pp.277-286.